Indian Journal of Pure & Applied Physics
Vol. 53, August 2015, pp. 521-529

Comparison of ZnO thin films on different substrates obtained by sol-gel process and deposited by spin-coating technique

W Chebil[1]*, A Fouzri[1,2], B Azeza[3], N Sakly[4], R Mghaieth[3], A Lusson[5] & V Sallet[5]

[1]Laboratoire Physico-chimie des Matériaux ; Unité de Service Commun de Recherche « High resolution X-ray diffractometer », Département de Physique, Université de Monastir, Faculté des Sciences de Monastir, Avenue de l'Environnement, 5019 Monastir, Tunisia

[2]Institut Supérieur des Sciences Appliquées et de Technologie de Sousse, Université de Sousse, Tunisia

[3]Laboratoire Micro-Optoélectroniques et Nanostructures, Faculté des Sciences de Monastir, Université de Monastir, Avenue de l'environnement 5019, Monastir, Tunisia

[4]Laboratoire Physico-chimie des Interfaces, Département de Physique, Université de Monastir, Faculté des Sciences de Monastir, Avenue de l'Environnement, 5019 Monastir, Tunisia

[5]Groupe d'Etude de la Matière Condensée, Centre National de la Recherche Scientifique/Université de Versailles Saint Quentin en Yvelines, UMR 8635, Paris France

*E-mail: Chbil.widad@live.fr

Received 14 November 2014; revised 14 January 2015; accepted 24 June 2014

In the present paper, zinc oxide thin films obtained by sol gel process and deposited on glass, sapphire, Si (100), Si (111) and ZnO substrates by spin-coating technique have been studied. Effects of using different substrates on the structural, morphological and optical properties have been investigated. The structural properties have been analyzed using X-ray diffraction (XRD) and the recorded patterns indicated that all the deposited films are polycrystalline with a hexagonal Wurtzite structure and exhibit preferentially oriented along the c-axis direction. The surface morphology has been examined by Scanning Electron Microscopy which revealed that the microstructure of the films strongly affected by the nature and orientation of substrate namely grain shape and size. Optical absorbance measurements have been taken using UV-Vis spectrophotometer and the calculated values of the direct band gap energy are around 3, 3.08 and 3.19 eV, for the ZnO films deposited on ZnO, sapphire c and glass substrates, respectively. Photoluminescence measurements taken at 4 K exhibit a near band edge composed by two principal's peaks situated at 3.36 and 3.31 eV and attributed to the neutral donor bound exciton (D°X) and to the deep acceptor (A°X), their intensity varied with the nature of substrate.

Keywords: ZnO, Thin film, Sol gel, Spin coating, Structural properties, Optical properties, Morphological properties

1 Introduction

The synthesis and characterization of ZnO nanostructures have been studied by many researchers due to the almost exclusive properties of ZnO such as wide direct band gap[1] (E_g = 3.37 eV), no toxicity[2], high transparency in Vis/near IR spectral region[3], excellent thermal stability[4] and the unique electrical and optoelectronic property of a large exciton binding energy (60 meV) at room temperature[5]. Owing to these properties zinc oxide have been studied widely for various applied devices including light emitting diodes[6] (LED), solar cells[7], optical waveguides[8], piezoelectric transduction[9], surface acoustic wave devices[10], conductive gas sensors[11] and varistors[12]. These properties and potential applications make this material an attractive subject for theoretical and experimental studies. ZnO thin films have been obtained using several techniques such as pulsed laser deposition[13] (PLD), chemical vapour deposition[14] MOCVD, Spray Pyrolysis[15], *dc* magnetron sputtering[16] and sol-gel technique[17,18]. The sol-gel method has distinct potential advantages over these other techniques due to its lower crystallization temperature, ability to tune microstructure via sol-gel chemistry, conformal deposition ability, compositional control and large surface area coating capability[19,20].

Selection of substrate materials which ZnO film is grown is necessary for the realization of exciton based photonic devices. The difference in lattice parameters and crystalline structures between ZnO and substrate materials may significantly affect the growth behaviour of ZnO film.

In the present study, ZnO thin films were obtained by sol gel process and deposited by spin coating

technique on glass, ZnO, sapphire (001) and *p*-Si (001) and (111) substrates.

Bulk ZnO substrates are clearly better choices as there is no lattice mismatch or thermal expansion coefficient difference. Glass is cheap and is widely used as substrates. To integrate ZnO devices into the Si technology, Si is chosen as substrate. Due to its physical, chemical and economical parameters basal plane sapphire has turned out to be also an appropriate substrate. The effect of using different nature and orientation of substrate on structural, morphological and optical properties of ZnO thin films have been investigated.

2 Experimental Details

Zinc acetate dehydrate (Zn $(CH_3COO)_2$ H_2O), isopropanol and monoethanolamine (MEA) were used as precursor, solvent and stabilizer, respectively. Zinc acetate was first dissolved in isopropanol at room temperature. When the solution turned milky, monoethanolamine was added in and then the resulting mixture was stirred at 50°C for 1 h to yield a clear and homogeneous solution. The molar ratio of MEA to zinc acetate was fixed at 1. The solution is used after aging at room temperature for 48 h. Before deposition, substrates were cleaned with acetone, ethanol, and deionized water successively in an ultrasonic bath. The films were deposited on different substrates by spin coating at room temperature with a rate of 2500 rpm for 30 s. After each coating, the as-deposited films were dried at 300°C in air for 10 min to evaporate the solvent and remove the organic component in the film. The coating and drying procedures were repeated twenty times to increase the film thickness. Finally, all the films were annealed in ambient atmosphere at 700°C. On the other side,temperature is not exceeded 500°C for the glass substrate, because there is a risk of a possible thermal fusion. Figure 1 shows the process for preparing ZnO sol gel and thin film. The measurement of thickness has been carried out using a Nano-calc 2000 (UV-Vis Lights). To properly get homogeneous thickness and good oscillation, measurement of thickness at different positions in the film has been done. The result showed that our samples have a thickness about 1.2 μm for the twenty thin layers deposition. After film deposition, crystal structure has been investigated by XRD (Bruker D8) with Cu K_α radiation (λ = 1, 5406 Å). The surface morphologies of films were evaluated by scanning electron microscope (SEM). The absorbance spectrum was observed using a UV-Vis DR/4000U spectrophotometer. The PL experiments were carried out using the 351 nm line excitation from an argon laser. The PL spectra were recorded at room and liquid helium temperature (4 K).

3 Results and Discussion

3.1 X-ray diffraction analysis

Figure 2 shows the XRD patterns of ZnO nanostructures grown on glass, sapphire, Si (100), Si (111) and ZnO substrates via the sol-gel method. The XRD spectrum of commercial ZnO powder (Sigma-Aldrich inventory: 1314-13-2) is also shown for comparison. The 2θ deposited on single-crystalline substrates (ZnO, Al_2O_3 and p-Si) reveal simultaneous presence of layer and substrate peaks. It was observed that all the deposited films were polycrystalline with a hexagonal wurtzite structure and exhibit good crystallinity as comparing to XRD pattern of ZnO powder but thin films had a preferential orientation along the c-axis. This is explained by the lowest surface energy density of the (002) plane of wurtzite crystal structure[21]. In the case of ZnO grown on ZnO, XRD pattern shows two very intense peak

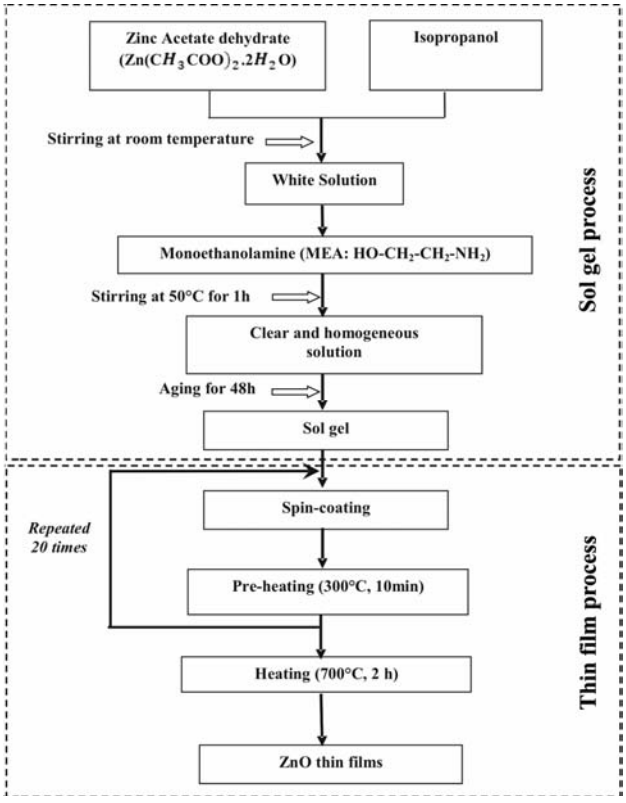

Fig. 1 — Process flow chart showing procedure for preparation of the sol-gel and thin films

corresponding to (002) and (004) reflexion of ZnO substrate as well as weak peaks attributable to (100), (101), (102), (110), (103) and (112) (Fig. 2e). But the (002) diffraction layer peak and the ZnO substrate peak overlap.

In order to describe the preferred c-axis perpendicular orientation, the relative intensities of (002) diffraction peak have been evaluated from $P=\{I(002)/[I(100)+I(002)+I(101)]\}$ according to the deposited substrate. The obtained values are given in Table 1. A better preferential orientation ($P \geq 0.92$) is reached for ZnO films deposited on *p*-Si substrates similar to that reported by Ghosh *et al*[22].

Table 1 — Crystallographic information for ZnO films grown on the different substrates and that of commercial powder ZnO

Substrate	2 θ(°) of (002) peak	P(002)	FWHM of (002) peak (°)	Average grain size D (nm)
Glass	34.44	0.677	0.455	20
Sapphire C	34.46	0.738	0.445	20
Si(111)	34.46	0.920	0.430	21
Si(100)	34.52	0.950	0.439	21
Commercial powder ZnO	34.53	0.193	0.194	48

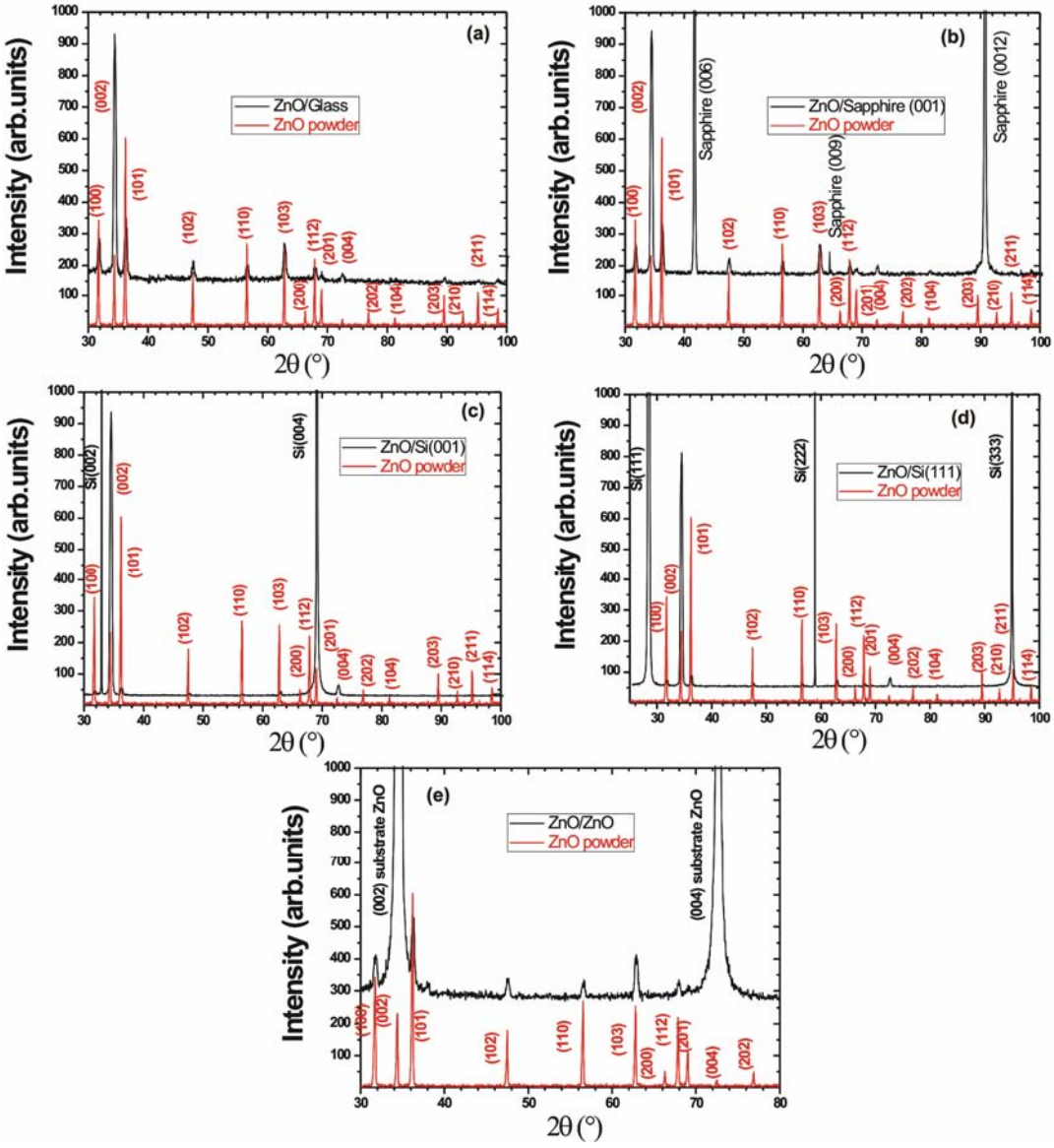

Fig. 2 — X-ray diffraction spectra of ZnO thin films grown on different substrates. XRD patterns of commercial ZnO are also drawn for comparison

The preferential orientation of ZnO thin films grown on different nature of substrates is strongly influenced by the precursor chemistry used and the heat-treatment procedures[23]. As well as Chia *et al*[24]. reported that the preheating temperature strongly affected the preferred orientation of ZnO films. In the present work, the experimental conditions appear more suitable for the highly growth along the c-axis orientation for the *p*-Si substrate than for the sapphire. But it cannot be compared with the ZnO layer deposited on ZnO substrate because of the ZnO (002) peak diffraction of layer and that of substrate overlap.

The average crystallite sizes of the films deposited at various substrates have been calculated using Scherrer's equation presented[25,26] as :

$$D = \frac{0.9\lambda}{\beta.\cos\theta} \qquad \ldots(1)$$

where λ (=1.5406 A°) is the wavelength of incident X-ray, β is the full width at half maximum (FHWM) measured in radians and θ is the Bragg angle of the highest diffraction peak. Note this formula is used in the approximation of spherical nanoparticles. The calculated results for (002) plane have been presented in Table 1. Practically no significant change in the crystallite size (~20 nm) is observed for the ZnO layers grown on different substrates but lower than the commercial powder. Grain size of ZnO deposited on sapphire substrate is close to those obtained by Srinivasan *et al*. (*D*=22 nm) using the sol gel process[27]. However, the grain size can be affected by other parameters such as temperature[28], nature of solvent[29], thickness[30], precursor concentration[31] …etc. The lattice constants '*a*' and '*c*' for ZnO layer deposited on different substrates are calculated and listed in Table 2 by using the following equation[32]:

Table 2 — Lattice parameters of ZnO films deposited on different substrates and those of commercial powder. For comparison lattice parameters of the JCPDS XRD database, file number 36-1451

Sample	Lattice parameters	
	a (Å)	*c* (Å)
ZnO/ glass	3.249	5.207
ZnO/sapphire	3.246	5.199
ZnO/Si(111)	3.243	5.199
ZnO/Si(100)	3.235	5.189
ZnO/ZnO	3.248	5.199
Commercial powder ZnO	3.240	5.188
ZnO powder JCPDS (N° 36-1451)	3.2498	5.2066

$$d_{hkl} = \left(\frac{4}{3}.\frac{h^2 + h.k + k^2}{a^2} + \frac{l^2}{c^2} \right)^{-1/2} \qquad \ldots(2)$$

Where d_{hkl} is the spacing between planes of given Miller indices *h*, *k* and *l*. The calculated lattice constants are in good agreement with JCPDS card 36-1451 and those of commercial ZnO powder. The little shift of the (002) diffraction peak of ZnO film (see Table 1) to higher 2θ angle in comparison with that in ZnO powder (2θ =34.53°) is attributed to first nucleation step which is very affected by lattice and thermal expansion coefficient mismatch of substrate surface.

3.2 Morphology of the ZnO films

To explore shape and size of ZnO nanostructure and their arrangement, Figs 3 and 4 show, respectively the SEM image of ZnO films grown on glass (a), sapphire (b), Si (100) (c), Si (111) (d), and ZnO (e) at 10^5 and 10^4 magnification. Variation in the surface morphology of the ZnO thin films with the nature and orientation of substrate namely grain shape and size is observed. The microstructure of the films grown on glass and sapphire shows a numerous nano-spherical grains but those grown on *p*-Si and ZnO substrates, the surface morphology is composed of a mixture of large and small nano-size crystallites. The nanostructures on Si and ZnO substrates consist of hexagonal structures (prisms and pyramids), differently located on the surface (perpendicular or parallel to the surface) and their mixed complexes, as a result of multi-nucleation. However, the formation of pyramids was clearer and located parallel to the normal of substrate in case of Si (111) and ZnO. In contrast, the facets of ZnO nanostructures for layer deposited on Si (100) are not visible. Upon the inspection of SEM image of ZnO on sapphire (Fig. 3b), some isolated pyramid ZnO nanostructures are seen which are due to the self texture character of growth, resulting in their c-axis texture. Sapphire, Si (111) and ZnO substrates have hexagonal surface structure which differs from that of Si (001). This explains why ZnO nanostructures are located with their c-axis perpendicular to the substrate surface and a high preferential c-axis orientation in XRD pattern.

For low magnification (10^4) (Figure 4), the SEM images show that the arrangement of ZnO nanostructure leads to mosaic structured ZnO layer on Si and ZnO substrate. But for glass and sapphire substrate, their arrangements appear in the form of

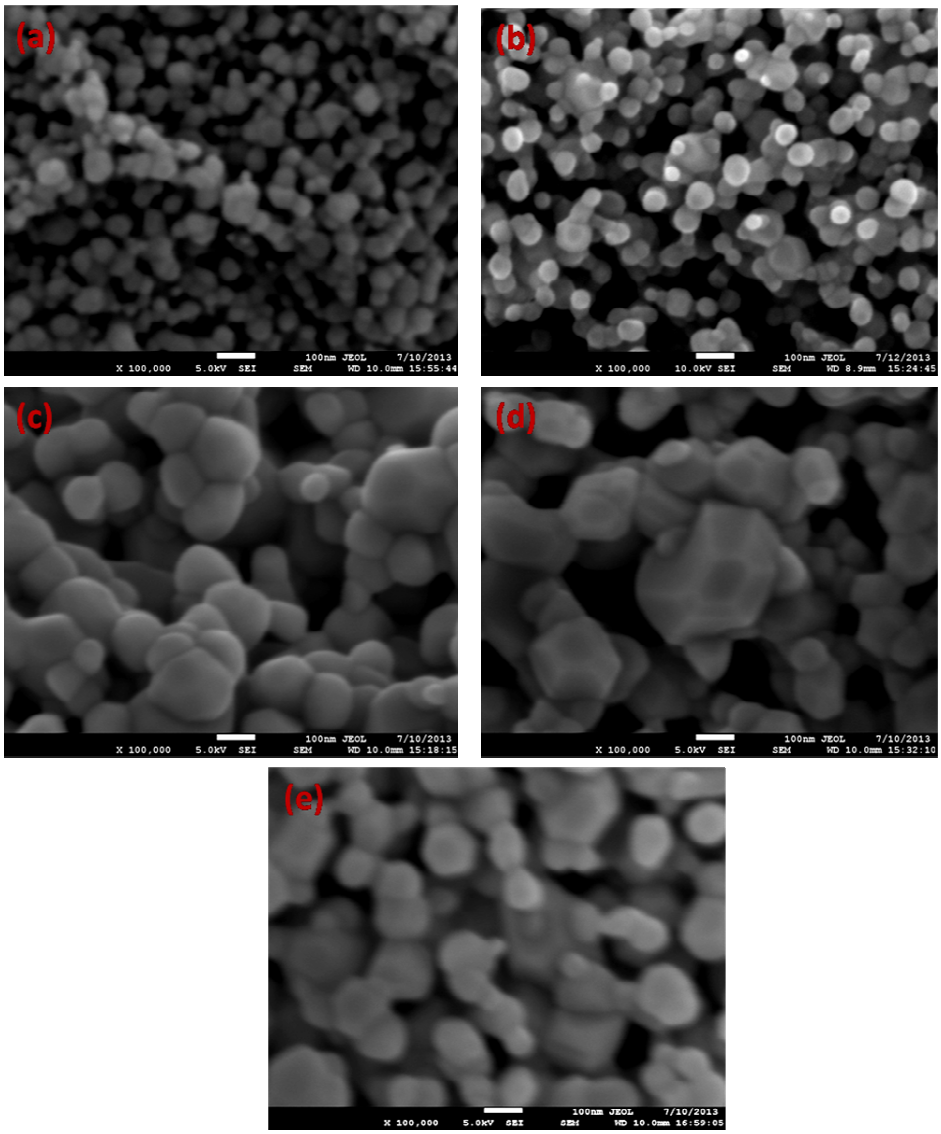

Fig. 3 — SEM images of the nanostructure ZnO film at 10^5 magnifications

domains which may be due to the substrate dictated growth and minimization of layer surface energy density.

3.3.1 UV-visible spectroscopy

To determine the optical band gap E_g, Tauc *et al.*'s plot[33] is used where the absorption coefficient α is a parabolic function of the incident photon energy ($E = h\nu$) and optical band gap E_g. This relation is given by:

$$\alpha = \frac{A(h\nu - E_g)^{1/2}}{h\nu} \qquad \ldots(3)$$

where A is a function of refractive index of the material, reduced mass and speed of light. The plot of $(\alpha E)^2$ as a function of the incident radiation energy for the ZnO thin films deposited on different substrates is shown in Fig. 5. The energy band gap is obtained from intercept of the extrapolated linear part of the curve with the energy axis. The values of energy band gap for the investigated samples has been found to be 3.19, 3.08 and 3.00 eV for the ZnO films prepared on the glass, sapphire and ZnO substrate, respectively. However, this technique cannot be used in the case of ZnO layer on Si substrate because its energy band gap (1.12 eV) is less than that of ZnO. The energy gap value obtained for ZnO on glass substrate is in good agreement with other reported values for example that found by Shankar *et al*[34]. (E_g= 3.19 eV) who used the

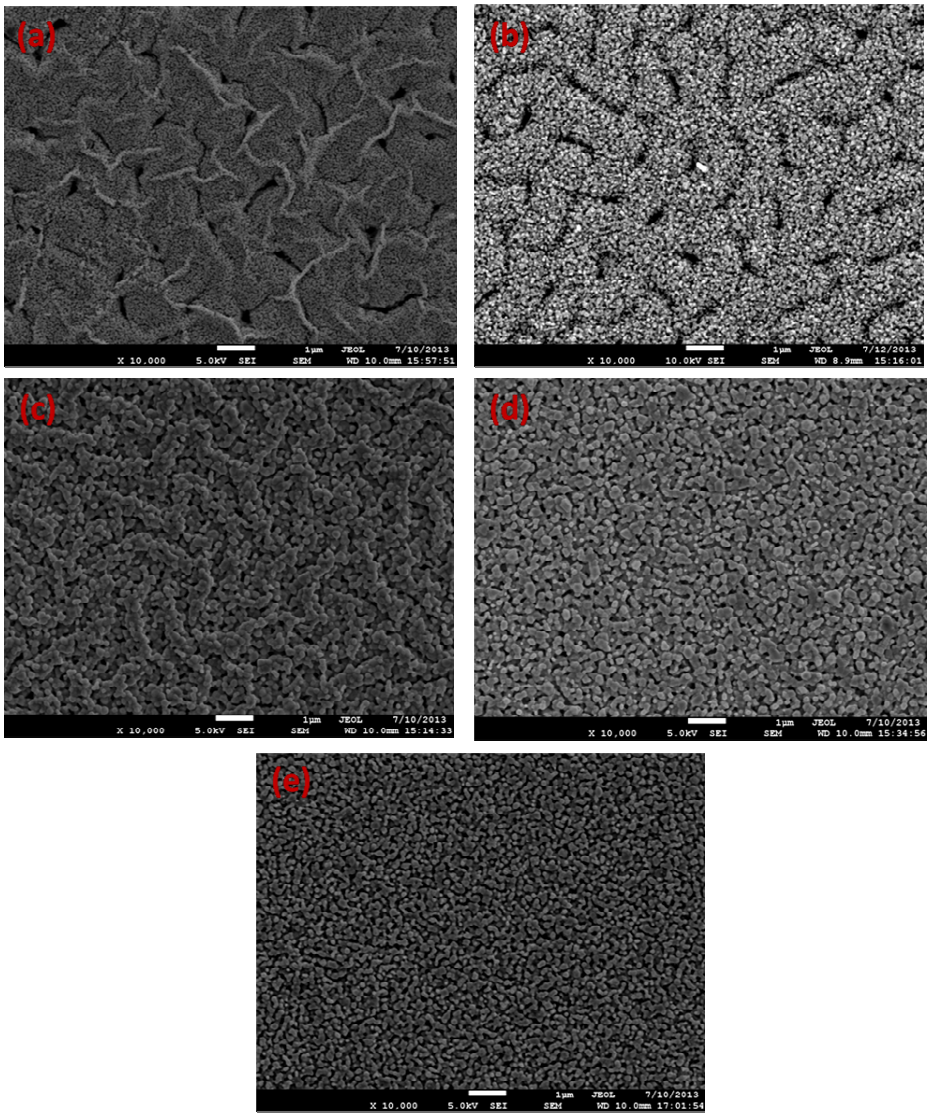

Fig. 4 — SEM images of the nanostructure ZnO film at 10^4 magnifications

same chemical precursor. The shift of the energy gap of ZnO deposited on sapphire and ZnO substrate can be explained by the defects as grain boundaries[35] and the less transparency of the substrate which causes a loss in the absorbing amount.

3.3.2 Photoluminescence measurements

Photoluminescence (PL) measurements of sample were performed at low and ambient temperature. At room temperature, no significant luminescence intensity is obtained from ZnO layers. However, in spectra of films deposited on Si (100) and sapphire substrate an ultraviolet (UV) emission peak at around 3.28 eV and a broad visible emission at around 2.3eV are seen. To evaluate the optical properties of the near band edge (NBE) emission of all the samples, PL was measured at (≈4 K) and the results are shown in Fig. 6. According to the previous studies[36,37], the band-edge PL in bulk ZnO can be divided into seven regions: free excitons (FE) excitons bound to ionized donors (D^+X), excitons bound to neutral donors (D^0X), excitons bound to neutral acceptors (A°X), exciton complexes with deep centers, two-electron transitions, and phonon replica region. Following this convention the emission line found at 3.36 eV and around 3.31 eV are, respectively attributed to the neutral donor bound exciton[38] (D°X) and to the neutral acceptor[39] (A°X).

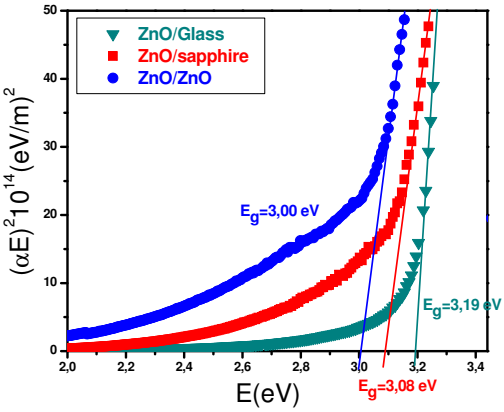

Fig. 5 — Plots of $(\alpha E)^2$ as a function of photon energy (E) for ZnO thin films grown on glass, sapphire and ZnO substrates

Samples grown on glass, sapphire and Si (111) have a relatively strong D°X peak indicating a high concentration of donors. The A°X for all the films is located between 3.315 to 3.320 eV as a consequence of different biaxial stresses in the thin films depending on the substrate.

The appearance of a shoulder around 3.30eV and a weak peak at 3.33 eV in case of ZnO grown on Si(001), Si(111) and ZnO may be dependent on the nature and orientation of substrate and thus on the crystalline quality of the thin films[40].At the low energy side, peaks situated at 3.23-3.24 eV have previously been identified as a donor-acceptor recombination[41] (DAP). This peak is accompanied by three different phonon replicas[42] with a period of 72

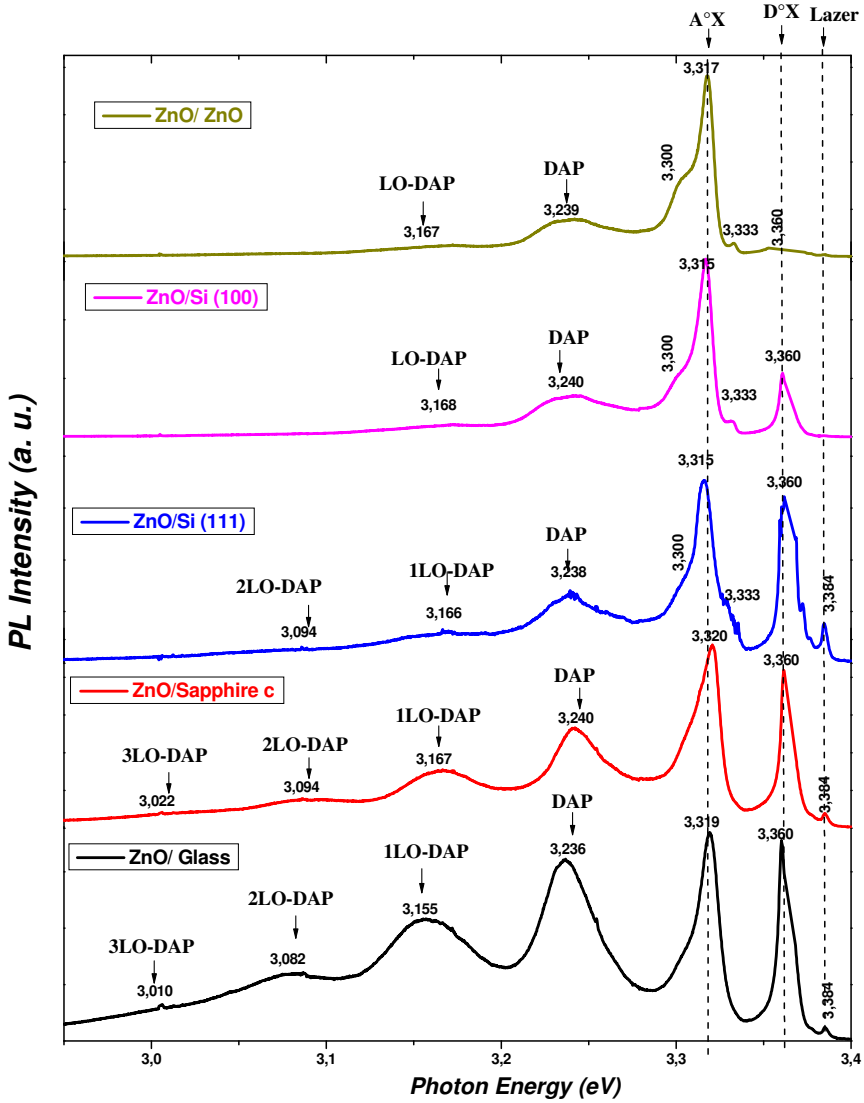

Fig. 6 — Near band edge emission region of ZnO thin films deposited on different substrates at 4 K

meV for layer grown on the glass and sapphire. But this number of replicas decreases for the other sample: we observe only a single phonon replica for ZnO layer on Si (100) and ZnO substrate. The variation in number of phonon replica can be due to the importance of interaction between phonon and defects in the thin films.

4 Conclusions

The present work is a comparative study between the ZnO thin films prepared by the sol-gel method in the same growth conditions but deposited on different substrates. The synthesized ZnO thin films exhibit a polycrystalline wurtzite structure with a preferential orientation along [001]. The grain morphology observed by SEM found to be strongly dependent on nature and orientation of the majority of substrates. Grains are nano-spherical on the glass and sapphire but they are in the form of hexagonal structures (prisms and pyramids). These nanostructures are located parallel to normal surface of Si and ZnO substrates. All the films show a near band edge which is composed by two principal peaks, situated at 3.36 eV and 3.31 eV and attributed to the neutral donor bound exciton (D°X) and to the deep acceptor (A°X), respectively. The intensity of donor bound exciton (D°X) decreases and practically disappears in the PL spectrum of ZnO on ZnO substrate, showing the low concentration of donors. There are intrinsic correlations between the structural, optical and morphological properties of the ZnO thin films, which are crucial for future study and application of piezoelectric devices and solar cells thin films.

References

1 Lin B, Fu Z & Jia Y, *Appl Phys Lett*, 79 (2001) 943.

2 Sahal M, Hartiti B, A Ridah, Mollar M & B Mar, *J Microelectronics*, 39 (2008) 1425.

3 Gopalakrishnan N, Balakrishnan L, Latha K & Gowrishankar S, *Crys Res & Tech*, 46 (2011) 361.

4 Malek M F, Mamat M H, Khusaimi Z, Sahdan M Z, Musa M Z, Zainun A R & Suriani A B, *J of Alloys & Compounds*, 582 (2014) 12.

5 Aksoy S & Caglar Y, *Superlattices & Microstructures*, 51 (2012) 613.

6 Jeong W J, Kim S K & Park G C, *Thin Solid Films*, 506 (2006) 180.

7 Hupkes J, Rech B, Kluth O, Repmann T, Zwaygardt B, Muller J, Drese R & Wutting M, *Solar Energy Materials & Solar Cells,* 90 (2006) 3054.

8 Jia C L, Wang K M, Wang X L, Zhang X J & Lu F, *Optics Express*, 13 (2005) 5093.

9 Tomar M, Gupta V, Sreenivas K & Mansingh A, *IEEE Trans on Device & Materials Reliability*, 5 (2005) 494.

10 Atanas J P, Asmar R A, Khoury A & Foucaran A, *Sensors & Actuators A*, 127 (2006) 49.

11 Rau U & Schmidt M, *Thin Solid Films*, 387 (2001) 141.

12 Mukae K, Tsuda K & Nagasawa I, *J of Appl Phys*, 50 (1979) 4475.

13 Sans J A, Segura A, Mollar M & Mari B, *Thin Solid Films*, 251 (2004) 453.

14 Kim K S, Kim H W & Lee C M, *Materials Sci & Engi B*, 98 (2003) 135.

15 Lee J H, Yeo B W & Park B O, *Thin Solid Films*, 457 (2004) 333.

16 Czternastek H, *Optoelectronics Rev*, 12 (2004) 49.

17 Natsume Y & Sakata H, *Thin Solid Films*, 372 (2000) 30.

18 Nagarani N & Vasu V, *J on Photonics & Spintronics*, 2 (2013) 19.

19 Luna-Arredondo E J, Maldonado A, Asomoza R, Acosta D R, Melendez-Lira M A & Olvera M de la L, *Thin Solid Films*, 490 (2005) 132.

20 Farley N R S, Staddon C R, Zhao L X, Edmunds K W, Gallagher B L & Gregory D H, *J of Materials Chem*, 14 (2004) 1087.

21 Zhang Y, Zheng H, Su J, Lin B & Fu Z, *J of Luminescence*, 124 (2007) 252.

22 Ghosh T, Dutta M & Basak D, *Materials Res Bulletin*, 46 (2011) 1039.

23 Ghosh R, Basak D & Fujihara S, *J of Appl Phys*, 96 (2004) 2689.

24 Chia C H, Tsai W C & Chou W C, *J of Luminescence*, 148 (2014) 111.

25 Rani S, Suri P, Shishodia P K & Mehra R M, *Solar Energy Materials & Solar Cells*, 92 (2008) 1639.

26 Lim W T & Lee C H, *Thin Solid Films*, 353 (1999) 12.

27 Srinivasan G, Kumar R T Rajendra & Kumar J, *Optical Materials*, 30 (2007) 314.

28 Ivanova T, Harizanova A, Koutzarova T & Vertruyen B, *Materials Lett*, 64 (2010) 1147.

29 Bari A R, Shinde M D, Deo Vinita & Patil LA, *Indian J of Pure & Appl Phys*, 47 (2009) 24.

30 Alias M F A, Aljarrah R M, Al-Lamy H K H & Adem K A W, *Int J of Appli or Innovation in Engi & Manag*, 2 (2013) 198.

31 Brien S O, Koh L H K, Copuroglu M & Crean G M, *M R S Proc*, 1035 (2008) 05.

32 Ghosh R, Basak D & Fujihara S, *J of Appl Phys*, 96 (2004) 2689.

33 Tauc J, Grigorvici R & Yanca Y, *Physica Status Solidi*, 15 (1966) 627.

34 Shankar S, Saroja M, Venkatachalam M, Muthukumarasamy N & Kumar V, *Int J of Innovative Res in Sci Eng & Tech*, 3 (2014) 8990.

35 Varnamkhasti M G, Fallah H R & Zadsar M, *Vacuum*, 86 (2012) 871.

36 Tomzig E & Helbig R, *J of Luminescence*, 14 (1976) 403.

37 Klingshirn C F, *Semicon Optics*, Springer, Berlin, (1995).

38 Teke A, Özgür Ü, Dogan S, Gu X & Morkoç H, *Physical Rev B*, 70 (2004) 195207.

39 Meyer B K, Alves H, Hofmann D M, Kriegseis W, Forster D, Bertram F, Christen J, Hoffmann A, Straburg M, Dworzak M, Haboeck U & Rodina A V, *Physica Status solidi*, 241 (2004) 231.

40 Heitsch S, Bundesmann C, Wagner G, Zimmermann G, Rahm A, Hochmuth H, Benndorf G, Schmidt H, Schubert M, Lorenz M & Grundmann M, *Thin Solid Films*, 496 (2006) 234.

41 PrzezdzieckaE, Wachnicki L, Paszkowicz W, Lusakowska E, Krajewski T, Luka G, Guziewicz E & Godlewski M, *Semicon Sci & Tech*, 24 (2009) 1.

42 Mandal S, Goswami M L N, Das K, Dhar A & Ray S K, *Thin Solid Films*, 516 (2008) 8702.